Future Technology
Open Access Journal
ISSN 2832-0379

August 2026| Volume 05 | Issue 03 | Pages 295-308

Journal homepage: https://fupubco.com/futech

https://doi.org/10.55670/fpll.futech.5.3.26

Future Publishing LLC

Article

Green cement production technology for reducing GHG emissions from the industrial sector of Kazakhstan

Ayagoz Khamzina[1], Teginbolat Samuratov[2], Ruslan Omirgaliyev[3], Anuar Aldongarov[4], Nurkhat Zhakiyev[5,6,7*]

[1]School of Digital Public Administration, Astana IT University, Astana, 010000, Kazakhstan
[2]Department of Energy Efficiency and Energy Saving, Ministry of Industry and Construction of the Republic of Kazakhstan, Astana, 010000, Kazakhstan
[3]School of Computer Science, Astana IT University, Astana, 010000, Kazakhstan
[4]Institute of Physical and Technical Sciences, L. N. Gumilyov Eurasian National University, Astana, 010000, Kazakhstan
[5]Davis Center, The Faculty of Arts and Sciences, Harvard University, Cambridge, MA, 02138, USA
[6]School of Intelligent Systems, Astana IT University, Astana, 010000, Kazakhstan
[7]Department of Physics, West Kazakhstan University, Uralsk 090000, Kazakhstan

ARTICLE INFO

Article history:
Received 09 January 2026
Received in revised form
21 May 2026
Accepted 27 June 2026

Keywords:
Federated learning, Silver economy,
Demand prediction, Financial technology,
Multi-platform behavioral data, Population aging

*Corresponding author
Email address:
nzhakiyev@gmail.com

DOI: 10.55670/fpll.futech.5.3.26

ABSTRACT

Reducing clinker and cement consumption is one of the key pathways to lowering CO_2 emissions from cement-related industrial processes. This study investigates the molecular interaction mechanism of an ester-based polycarboxylate ether (PCE) fragment with Ca^{2+} and SiO_2 as a simplified representation of PCE-assisted silica-fume systems and evaluates how such material-efficiency assumptions can be incorporated into Kazakhstan-specific greenhouse gas emission scenarios. Density functional theory calculations were performed using the B3LYP-D3/6-311++G(d,p) level of theory, followed by molecular electrostatic potential, non-covalent interaction, reduced density gradient, electron localization function, and QTAIM analyses. The results indicate that carboxylate oxygen atoms in the PCE fragment act as the main coordination sites for Ca^{2+}, while the SiO_2 model contributes additional oxygen-containing interaction sites. The ternary PCE–Ca^{2+}–SiO_2 system shows a more connected interaction network than the isolated PCE and PCE–SiO_2 systems, supporting the plausibility of Ca^{2+}-mediated adsorption and dispersion in silica-rich cementitious environments. In parallel, greenhouse gas emissions from Kazakhstan's Industrial Processes and Product Use sector were assessed under three scenarios: without measures, with current measures, and with additional measures. The additional-measures scenario incorporates material-efficiency assumptions related to optimized use of PCE–silica fume, clinker reduction, and process improvements. The results should be interpreted as a molecularly informed scenario framework. The study contributes to the discussion of green cement production technologies and industrial decarbonization pathways in Kazakhstan.

1. Introduction

Kazakhstan has become a major economic force in Central Asia, with development mainly propelled by the export of its vast fossil fuel resources, especially oil and natural gas. Kazakhstan ranks number seventeen in the world in oil production and number nine in coal production, making it a significant energy producer on the global market, as it is almost doubling its own energy demand [1]. Nonetheless, due to the severe climate and high dependence on fossil fuels, high energy intensity leads to a significant amount of greenhouse gas (GHG) emissions, making the country one of the largest emitters in Europe and Central Asia and one of the top 20 in the world in terms of per capita carbon dioxide (CO_2) emissions. According to the 2018 National Cadastral Report (NCR), Kazakhstan's GHG emissions in 2018 were 396.57 Mt of CO2 equivalent, 2.74 percent higher than in 1990. The

combustion of fossil fuels accounted for 73.47% of the total, with the rest coming from fugitive emissions (11.9%) and agriculture (9.2%) [2]. Kazakhstan has been engaged with the UNFCCC and has made bold commitments under the Paris Agreement to cut GHG emissions by 15 percent from 1990 levels by 2030 [3,4]. Since achieving these objectives requires far-reaching energy and industrial reforms, national plans should be based on sustainable solutions [5], such as new CO_2 capture techniques, such as calcium looping, which can significantly reduce emissions from cement plants [6]. One of the major sources of CO_2 emissions is cement production. The recent policy interventions in the country, as outlined in the national roadmap, indicate a growing desire to revamp the local cement industry. Of the 15 cement plants in the country, 12 already operate more energy-efficient dry processes, while the remaining three still use wet technology, which cannot be easily upgraded without substantial capital investment. Simultaneously, the reinforcement of the National Emissions Trading Scheme and the possible implementation of a carbon border adjustment have increased the pressure on the necessity of producing greener cement, which is important in case domestic producers are able to avoid increased costs and even close down in case of global competition and low carbon allowances [7]. Concrete consists of aggregates that provide bulk, and cement serves as the binding agent [8]. Since cement production requires heating $CaCO_3$ to high temperatures, it emits a large amount of CO_2. Others: Partial replacement of cement with superplasticizers, silica fume, and other chemical additives slows cement production and reduces carbon dioxide emissions, a significant contributor to greenhouse gas emissions [9-13].

Superplasticizers, with poly(carboxylate) ethers (PCEs) as the predominant example, are used to improve the workability of concrete and may also reduce cement consumption and increase mechanical performance [12,14-18]. Although PCEs, which are comb-shaped copolymers with an anionic backbone and neutral side chains, interact strongly with calcium ions, they also maintain favorable rheological properties. Silica fume further strengthens durability and compressive capacity [12,15-18]. Table 1 consolidates key studies on GHG mitigation within Kazakhstan's concrete sector, highlighting the importance of cement replacement through chemical additives. As the Technology Roadmap for the Low-Carbon Cement Industry outlines strategies for emissions reduction through innovative technologies and policy reforms, it emphasizes a shift toward dry cement processing and the use of alternative fuels [7]. Accurate data on carbon factors is vital for emerging economies [19]. The Carbon Emission Factors in the Cement Industry report emphasizes the importance of accurate assessments for newly industrialized regions and provides a basis for evaluating the impact of cement replacement strategies.

Enhanced material efficiency can support ecologically responsible building practices, according to a study on green building development in Kazakhstan, which identifies several factors influencing sustainable construction. The total carbon footprint of a structure decreases with lower cement content. When combined, these results provide a strong foundation for investigating how chemical admixtures, such as plasticizers and silica fume, can reduce greenhouse gas emissions during concrete manufacturing in Kazakhstan. The work uses density functional theory (DFT) studies to reveal the connections among PCEs, calcium ions, and silica fume, aiming to bridge the gap between molecular-level insights and large-scale emissions forecasts. The paper also discusses the environmental and economic impacts of cement substitution in Kazakhstan's industrial infrastructure, which aligns with national policy to curb greenhouse gas emissions. Estimates from Kazakhstan's National Inventory Data suggest that the environment will be affected more broadly, and DFT modeling provides extensive data on the molecular interactions between PCEs and silica fume. This is an integrated approach that incorporates macroscopic and microscopic viewpoints in the analysis of sustainable concrete mixtures. These admixtures will help achieve better performance and emissions reductions, which are also applicable to Kazakhstan's climate goals. In this respect, the results contribute to the development of more sustainable construction materials.

Table 1. Recent works on reducing GHG emissions in Kazakhstan

Study Focus	Methodology	Key Findings	Year
Technology Roadmap for Low-Carbon Cement Industry	Developed scenarios for low-carbon development, including transition to dry cement technology and use of alternative fuels.	Expected improvements in energy efficiency and CO_2 reduction through technology upgrades and policy measures.	2016 [7]
Carbon Emission Factors in the Cement Industry	Analyzed carbon emission factors in emerging economies.	Highlighted the need for accurate emission factors to assess reduction strategies.	2023 [19]
Green Building Development in Kazakhstan	Examined factors influencing green building development.	Identified opportunities for sustainable construction practices, including material efficiency.	2021 [20]
Role of Concrete in Life Cycle GHG Emissions	Investigated life cycle emissions of buildings and pavements.	Emphasized the impact of concrete production on overall emissions.	2021 [21]

To date, no research has used Quantum Theory of Atoms in Molecules (QTAIM), Non-Covalent Interaction (NCI), and Reduced Density Gradient (RDG) analyses with DFT to explore the molecular behavior of superplasticizers with silica fume and calcium ions. This study combines atomistic insights with national-scale CO_2 emission forecasts for Kazakhstan, providing a molecularly informed scenario framework to evaluate assumptions about cement-related emissions. Our approach includes an analysis of DFT results including molecular electrostatic potential maps (MEPs), reduced density gradients (RDG), noncovalent interaction analyses (NCI), electron localization functions (ELF), and critical points for intermolecular interactions of PCE superplasticizer with calcium ion in the presence of silica fume and forecasting of greenhouse gases emissions in industrial process and product use sector of Kazakhstan under without measures (WOM), with current measures (WCM), and with advanced measures (WAM) (advanced measure based on partial replacement of cement with superplasticizer) scenarios. As the Technology Roadmap for the Low-Carbon Cement Industry outlines strategies for emissions reduction through innovative technologies and policy reforms, it emphasizes a shift toward dry cement processing and the use of alternative fuels. Accurate data on carbon factors is vital for emerging economies.

The Carbon Emission Factors in the Cement Industry report emphasizes the importance of accurate assessments for newly industrialized regions and provides a basis for evaluating the impact of cement replacement strategies. Enhanced material efficiency can support ecologically responsible building practices, according to a study on green building development in Kazakhstan, which identifies several factors influencing sustainable construction. The total carbon footprint of a structure decreases with lower cement content. The findings justify additional research into the extent to which chemical admixtures, such as plasticizers and silica fume, can reduce greenhouse gas emissions from concrete production in Kazakhstan. The interactions among PCEs, calcium ions, and silica fume were investigated using density functional theory (DFT), thereby linking molecular-scale behavior to emissions-related projections at the production level. The paper also considers the environmental and economic impacts of partial cement replacement in industrial settings in Kazakhstan. Using the National Inventory Data of Kazakhstan as a basis for forecasting suggests broader environmental impacts, and DFT simulations help elucidate the mechanism of action between silica fume and PCEs.

This approach presents a unique blend of microscopic and macroscopic perspectives, paving the way for groundbreaking improvements in sustainable concrete mixtures. Because these admixtures optimize performance while curtailing emissions, they play a vital role in advancing Kazakhstan's climate-related objectives. Such innovation underpins sustainable construction worldwide. Two specific research gaps are addressed in this work. First, the local role of Ca^{2+}-mediated interaction between an ester-based PCE fragment and a simplified SiO_2 model has not been sufficiently quantified using a combined molecular electrostatic potential (MEP), non-covalent interaction (NCI), reduced density gradient (RDG), electron localization function (ELF), and Quantum Theory of Atoms in Molecules (QTAIM) framework. Second, the implications of such molecular-level interaction mechanisms have rarely been translated into transparent, Kazakhstan-specific IPPU emission scenarios that include explicit assumptions about cement substitution, clinker reduction, and technology adoption. Accordingly, this study develops an integrated molecular-to-scenario framework for evaluating green cement production technology in Kazakhstan. DFT is used as mechanistic support for literature- and scenario-based assumptions concerning PCE-assisted silica-fume cement systems. The specific objectives are: to construct a simplified but chemically interpretable DFT model of an ester-based PCE fragment interacting with Ca^{2+} and SiO_2; to characterize intermolecular interactions using MEP, NCI/RDG, ELF, and QTAIM descriptors; to define WOM, WCM, and WAM scenarios for Kazakhstan's IPPU emissions using explicit equations and assumptions; to explain how molecular interaction evidence can inform, but not replace, scenario assumptions for clinker and cement reduction.

2. Materials and methods

2.1 DFT methodology

SiO_2 was selected as a simplified computational representation of the reactive oxygen-containing sites of silica fume, while Ca^{2+} ions were introduced as the main calcium-mediated adsorption species involved in PCE coordination in cementitious environments. This reduced model was designed to represent local PCE–Ca^{2+}–SiO_2 interactions rather than the full mineralogical complexity of hydrated cement paste. The SiO_2 model was constructed as a minimal molecular unit to isolate local interactions between the silica-related oxygen sites, Ca^{2+}, and PCE functional groups. Therefore, the model does not reproduce an extended amorphous silica surface, surface heterogeneity, silanol density, particle-scale effects of commercial silica fume, or the complete pore-solution chemistry of cement paste. The simplified model also does not explicitly include tricalcium silicate (C_3S), dicalcium silicate (C_2S), calcium silicate hydrate (C-S-H), aluminate phases, sulfate species, alkali ions, or the high ionic strength of cement pore solution. These omissions are acknowledged as limitations of the DFT component. The purpose of the calculation is to obtain molecular-level evidence on local coordination and adsorption tendencies, not to simulate the complete cement matrix. An ester-based polycarboxylate ether (PCE) molecular fragment was selected as the computational model (Figure 1).

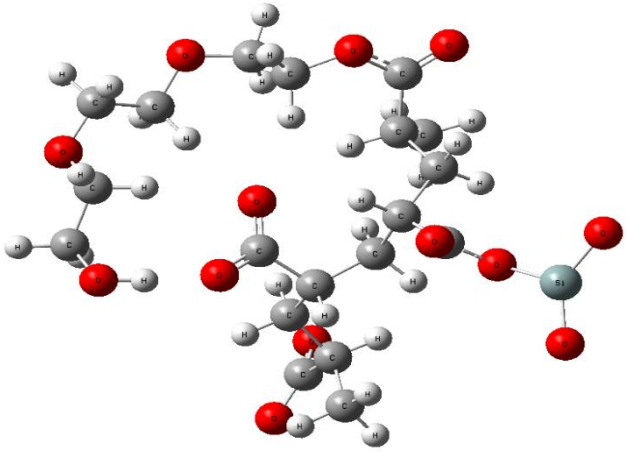

Figure 1. 3D representation of PCE superplasticizer

This model is a fragment of a repeat unit of the model and not a commercial high-molecular-weight PCE polymer. It features three carboxylic/carboxylate groups and a polyethylene-glycol-type side chain, which are essential groups for Ca^{2}+/cation coordination, electrostatic adsorption, steric stabilization, and interaction with oxygen-containing mineral surfaces. The optimized structure contains 61 atoms (C, H, and O), and its Cartesian coordinates are provided in the Supplementary Information. The commercial PCEs are comb-shaped polymers with various molecular weights, side-chain lengths, and carboxylate distributions, and a full polymer chain would be too large to treat directly with DFT. Thus, the present molecular fragment was employed to probe local adsorption and coordination behavior at the atomistic level. The −3 charge state was assigned by deprotonating three carboxylic acid groups in the PCE fragment, yielding three carboxylate sites capable of coordinating Ca^{2}+. This protonation state was chosen as a chemically reasonable approximation for the alkaline limit. Cement pore solutions are alkaline with pH values of typically around 12.5-13.5. Under these pH conditions, the carboxylic groups of acrylic- and methacrylic-acid-based groups are likely to be mostly deprotonated as their pKa values are several units below the pH of the pore solution. The side chain of polyethylene-glycol was left neutral with ether and alcohol groups, since it is not likely to deprotonate in the normal alkaline cement pore-solution environment. The −3 PCE fragment and Ca^{2}+ give a net complex charge of −1 in the PCE–Ca^{2}+-SiO_2 ternary system. It is important to note that this

charge assignment is an approximation to the alkaline-limit protonation state and that other protonation states should be explored in future studies.

All DFT calculations were carried out in the gas phase (no implicit solvent model). This was done to enable efficient geometry optimization and detailed electronic-structure analysis of the investigated complexes and to isolate the intrinsic PCE–Ca^{2+}–SiO_2 interactions. Real cement pore solutions, however, are aqueous, highly alkaline, and ion-rich, and solvation, ionic strength, and explicit water molecules may affect adsorption energies, hydrogen-bonding patterns, and Ca^2+ coordination. The lack of PCM/SMD solvent treatment and the explicit water molecules are thus recognized as limitations of the present study. DFT calculations were made to examine the intermolecular interactions between the ester-based PCE fragment, Ca^2+ ions, and the simplified SiO_2 model. The calculations were performed using the B3LYP functional [22,23] with the 6-311++G(d,p) basis set and the Grimme D3 dispersion correction to account for dispersion contributions to noncovalent interactions. All calculations were done using Gaussian 09 Rev. E.01 [24]. The optimized structures and electronic descriptors were visualized and post-processed using GaussView 6.0 [25], Multiwfn 3.7 [26] and VMD 1.9.1 [27]. Firstly, we acquired optimized structures of the PCE superplasticizer. Next, these structures were employed to model PCE monomer complexes with SiO_2 with and without the presence of Ca^{2+} ions. We used a charge of -3 on the ester-based PCE monomers in our simulations. Frequency calculations were performed to ensure that the optimized structures were global energy minima (i.e., had no negative frequencies). To interpret the DFT results, MEP maps, RDG plots, NCI analyses, ELF plots and critical point analyses were generated. The combination of these techniques was used to describe the intermolecular interaction between PCE superplasticizer and the calcium ions in the presence of micro-silica.

The B3LYP-D3/6-311++G(d,p) level of theory was chosen since it offers a good compromise between computational effort and accuracy for organic–inorganic clusters with PCE fragments, Ca^{2+} and SiO_2. To account for weak adsorption contacts, hydrogen bonding, and other noncovalent interactions, the D3 dispersion correction was applied. While more recent functionals such as ωB97XD and M06-2X may be more accurate for selected noncovalent systems, the purpose of the present work was to compare interaction patterns using the same set of simplified molecular models. This is recognized, and future work will include benchmark calculations for several key structures using range-separated or meta-hybrid functionals. In the main calculations, the BSSE correction was not applied, since the present study emphasizes relative electronic descriptors and topological trends rather than absolute adsorption energies. This omission is mentioned as a limitation. Further studies should involve counterpoise-corrected interaction energies and comparisons to ωB97X-D, M06-2X, or correlated wave-function methods for a subset of structures.

2.2 Forecasting of greenhouse gas emissions analysis

The historical emissions dataset was obtained from Kazakhstan's National Inventory Document, submitted to the UNFCCC on 30 December 2024. The relevant inventory basis is "Industrial Processes and Product Use", where IPPU emissions are reported according to the CRT/IPCC categories. A special attention is paid to "Mineral Industry (CRT category 2.A)", "Cement Production (CRT category 2.A.1)", and the methodology for estimating emissions from other uses of carbonates under (CRT category 2.A.4.d), because the production of cement and the use of carbonate are the inventory categories where the production of clinker, the calcination of limestone, and cement-related process emissions are included in the national GHG inventory [28]. The time series for model calibration spans 1990-2022, aligning with Kazakhstan's national inventory submitted under the UNFCCC transparency framework. The NID-reported IPPU categories are thus used as a basis for the model, and assumptions are made for the different pathways of WOM, WCM, and WAM. The forecasting component was developed as a scenario-based linear trend extrapolation using historical CO_2-equivalent emissions from Kazakhstan's Industrial Processes and Product Use (IPPU) sector. For each selected inventory category, the baseline time-trend model was specified (Eq.1):

$$E(k,t) = \alpha k + \beta kTt + \varepsilon(k,t) \quad (1)$$

where E(k,t) is the annual CO_2-equivalent emission level of inventory category k in year t, Tt is the time-trend variable, αk is the intercept, βk is the annual trend coefficient, and ε(k,t) is the residual term. The model was calibrated for the 1990–2022 period and then used as the baseline pathway for constructing WOM, WCM, and WAM scenarios.

A time-trend model is used because harmonized annual data are lacking for cement production, clinker factor, plant-level technology adoption, silica fume use, PCE dosage, and cement-specific industrial output. Hence, these variables (GDP, population, cement demand, and industrial output) are treated as contextual variables but are not tested statistically as explanatory variables in the present model. The model should be considered as a clear scenario projection, not as a multivariate econometric model with causal relationships. For total IPPU emissions, the estimated model produced α = −639,794.256, β = 329.324 kt CO_2-eq/year, R^2 = 0.624, RMSE = 2,435.68 kt CO_2-eq, $p < 0.001$, and a 95% confidence interval for β of 235.62–423.02 kt CO_2-eq/year. For the mineral industry category 2A, the model produced α = −498,062.408, β = 250.529 kt CO_2-eq/year, R^2 = 0.857, RMSE = 976.11 kt CO_2-eq, $p < 0.001$, and a 95% confidence interval for β of 212.98–288.08 kt CO_2-eq/year. These statistics describe the historical trend fit only and are not interpreted as evidence of causal prediction (Table 2). A simple backtesting approach was also used by fitting the model to 1990–2017 data and testing it against observed emissions for 2018–2022. The total IPPU emissions and mineral industry emissions back-testing RMSE were 1,493.04 kt CO_2-eq and 723.08 kt CO_2-eq, respectively. This validation step shows that the trend model is appropriate to compare indicative scenarios.

The WOM scenario is a counterfactual baseline scenario with no additional mitigation measures beyond the historical emission trend. It does not assume the implementation of a specific clinker-reduction policy, nor the promotion of PCE-silica-fume systems, nor a specific effect of cement substitution due to the use of technology. Emissions thus follow the "baseline time-trend projection" based on past IPPU inventory data. Only officially planned and implemented measures are included in the WCM scenario. The policy basis for this scenario is the Concept for the Transition of the Republic of Kazakhstan to a Green Economy and the Action Plan for the Implementation of the Green Economy Concept for 2024–2030, approved by Government Decree No. 1019 of 29 November 2024.

Table 2. Regression diagnostics for the baseline time-trend model

Series	α / inter-cept	β/slope, ktCO_2eq /year	R^2	RMSE, kt CO_2-eq	95% CI for β	Back-testing RMSE
Total IPPU emissions	-639,794.25	329.324	0.624	2,435.68	235.62–423.02	1,493.04
Mineral industry	-498,062.41	250.529	0.857	976.11	212.98–288.08	723.08

Table 3. Scenario assumptions for WOM, WCM, WAM

Parameter	WOM	WCM	WAM base case
Historical basis	NID 1990–2022 IPPU time series	NID 1990–2022 IPPU time series	NID 1990–2022 IPPU time series
Projection model	Linear time-trend baseline	Linear time trend adjusted by implemented/ planned measures	WCM pathway plus additional PCE–silica-fume technology term
Policy status	No additional measures	Implemented/ planned measures only	Additional/proposed technology measure
PCE–silica-fume adoption rate A(2040)	0%	0% as separate measure	70%
Clinker/cement reduction in adopted mixes Rclinker.	0%	0% as separate PCE–silica-fume measure	10%
Cement-related share of mineral-industry emissions Scement.	Not applied	Not applied	80%
Effective additional mineral-industry reduction in 2040	0%	0% relative to WCM	5.6% relative to WCM
Main interpretation	Counterfactual baseline	Current/planned policy pathway	Technology-enhanced mitigation pathway

The relevant policy elements are “Energy saving and energy efficiency”, Target indicator 7 “Energy intensity of GDP to be reduced by 15% by 2030 from 2021”, and measure 28 “Implementation of energy saving and energy efficiency measures by industrial enterprises” and measure 31 “Promotion and stimulation of innovative technologies through interaction between science and production”. The WCM scenario also covers the fifth section of the 2024–2030 Action Plan, namely measure 50 on the phased transition of category I enterprises to best available techniques with integrated environmental permits and measure 51 on automated monitoring systems for atmospheric emissions by category I enterprises. These measures are considered de facto or officially planned. Thus, WCM incorporates general industrial energy-efficiency improvements and BAT-related modernization, but does not consider accelerated adoption of PCE–silica fume as a standalone cement-substitution pathway.

The WAM scenario is based on WCM and includes proposed technology-related measures that are not considered as implemented policy. In the present study, the extra WAM measure is the adoption of optimized PCE–silica-fume cement systems to reduce clinker/cement use in the mineral industry. This assumption is in line with Kazakhstan's overall policy approach in the field of industrial energy efficiency, innovation, and best available techniques, but is not expressed as a standalone measure in the Green Economy Action Plan (Table 3). To maintain consistency in the inventory, the extra WAM mitigation term was applied only to the cement sector within the mineral sector in NID [28, p.221]. It was not indiscriminately applied to the whole IPPU sector.

This distinction is required because IPPU covers other industries (chemical industry, metal industry, non-energy products from fuel and solvent use, substitutes for ozone-depleting substances, etc.) that are not directly related to PCE–silica-fume cement optimization. The WAM mitigation term for the mineral industry was determined (Eq.2):

$$E(2A,t,WAM) = E(2A,t,WCM) \times [1 - A(t) \times Rclinker \times Scement] \quad (2)$$

where E(2A,t,WCM) is the mineral-industry emission level under WCM, A(t) is the assumed adoption rate of the PCE–silica-fume approach, Rclinker is the clinker/cement reduction fraction in adopted mixes, and Scement is the cement-related share of mineral-industry emissions. In the base WAM assumption, A(2040) = 70%, Rclinker = 10%, and Scement = 80%, resulting in an effective 5.6% additional reduction relative to the WCM mineral-industry pathway in 2040. The conceptual role of PCE–silica-fume optimization in concrete production is shown in Figure 2. Superplasticizers are not used directly as a cement replacement but are used to enhance dispersion and workability, which can help reduce the water-to-cement ratio and allow the use of supplementary cementitious materials such as silica fume. This mechanism is operationalized in the WAM scenario in the present study by making explicit assumptions about the adoption rate, the reduction in clinker use, and the cement-related share of mineral-industry emissions.

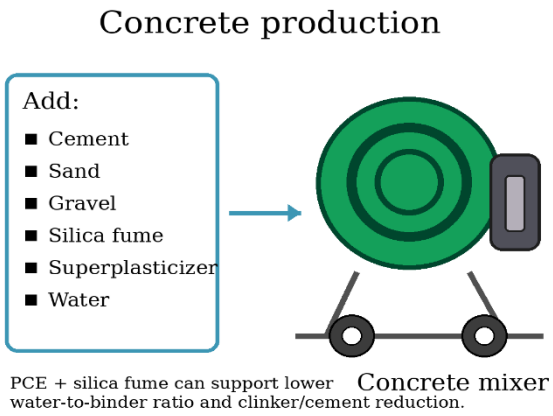

Figure 2. Concrete production process

3. Results and discussion

3.1 MEPS map

Figure 3 presents MEP maps for three systems: isolated PCE, PCE–SiO_2, and PCE–Ca^{2+}–SiO_2. MEP identifies regions of electrostatic complementarity—electron-rich (negative, red) and electron-deficient (positive, blue) areas—that predict susceptibility to electrostatic interactions such as hydrogen bonding, ionic coordination, and dipole–dipole forces. In the PCE system, strong negative potential concentrates around the carboxylate ($-COO^-$) groups, identifying these as the primary nucleophilic sites for adsorption onto positively charged cementitious surfaces (e.g., Ca^{2+} ions).

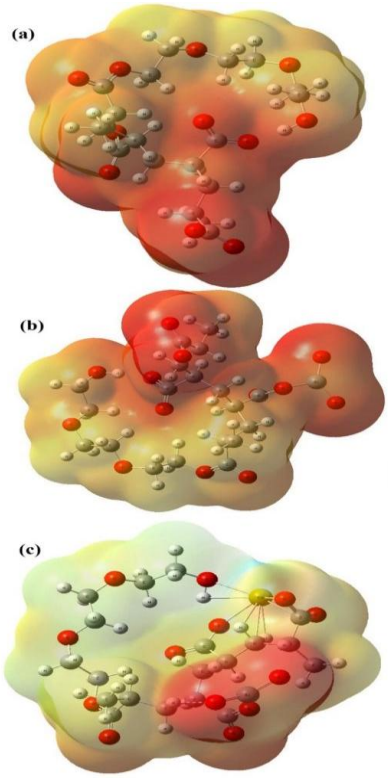

Figure 3. MEPs for PCE superplasticizer (a), PCE superplasticizer with SiO_2 (b), and PCE superplasticizer with calcium and SiO_2 (c). Color scale bar (from –0.05 to +0.05 a.u.) and isovalue = 0.0004 a.u.

This distribution explains the dispersive function of PCE in fresh concrete. In the PCE–SiO_2 system, the introduction of SiO_2 slightly perturbs the potential distribution. Oxygen atoms on the silica surface exhibit increased potential gradients, indicating enhanced polarity at the PCE–silica interface. This trend suggests favorable silanol–carboxylate hydrogen bonding, which may influence particle dispersion and agglomeration behavior. In the PCE–Ca^{2+}–SiO_2 system, a new, highly concentrated positive region appears around the Ca^{2+} ions, while a strong negative potential persists on the carboxylate groups. This electrostatic complementarity confirms that Ca^{2+} acts as an ionic bridge between the anionic PCE and the silica surface, creating a cooperative binding network involving both ionic coordination and hydrogen bonding. MEP maps electrostatic complementarity, predicting where interactions are likely to occur. It does not prove their existence or strength; that requires the complementary analyses below (NCI, RDG, ELF, QTAIM).

3.2 NCI analysis

NCI isosurface maps are shown for the three systems in Figure 4.

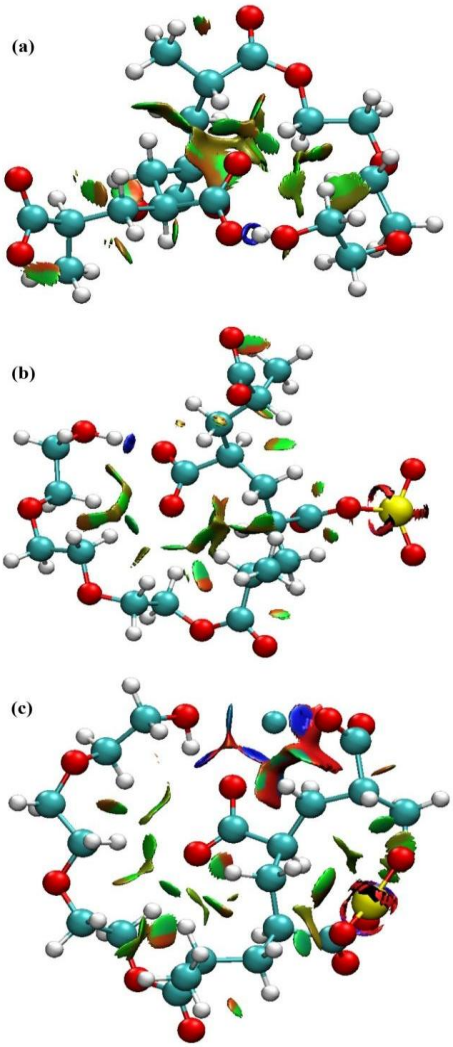

Figure 4. NCIs for PCE superplasticizer (a), PCE superplasticizer with SiO2 (b), and PCE superplasticizer with calcium and SiO2 (c). Isovalue = 0.5 a.u. with color scale: blue (attractive, sign(λ_2)ρ < –0.02), green (van der Waals, –0.02 to 0.02), red (repulsive, >0.02).

NCI is not an electrostatic potential like MEP, but rather it displays the spatial distribution and character of weak intermolecular interactions (hydrogen bonds, van der Waals forces, steric clashes) using a color scale: blue = strong attractive (hydrogen bond / ionic coordination), green = weak attractive (van der Waals), red = repulsive (steric). In the PCE system, there are some weak intramolecular van der Waals contacts, which are manifested by the presence of scattered green isosurfaces around the carboxylate and ether oxygen atoms. No blue surfaces are found, indicating the absence of strong attractive interactions in the isolated molecule. New blue and green isosurfaces appear at the PCE–silica interface in PCE–SiO_2 system.

Hydrogen-bond-like attractive interactions are shown as blue regions between carboxylate groups and silanol (–SiOH) sites. Green surfaces are regions of weaker van der Waals contacts along the polymer backbone. This evidence indicates that silica particles provide additional adsorption sites that improve the dispersion of PCE. The interaction pattern is much more pronounced in the vicinity of the Ca^{2+} ions in the PCE–Ca^{2+}–SiO_2 system. The Ca^2+ isosurfaces are dense to link Ca^2+ to the negatively charged carboxylate oxygens of PCE, and other blue surfaces are used to link Ca^{2+} to silanol groups on SiO_2. No red (repulsive) surfaces are observed, indicating that the intermolecular network is stable and cooperative. NCI is used to visualize the location of non-covalent interactions and the type (attractive H-bond/ionic vs. weak van der Waals vs. repulsive). In contrast to MEP (which only predicts electrostatics) and RDG (which quantifies strength distribution), NCI gives direct spatial mapping of interaction zones.

3.3 RDG plot

Figure 5 presents RDG scatter plots for the three systems. While NCI maps the spatial distribution of interactions, RDG quantifies their strength distribution via the function RDG versus sign(λ_2)ρ. In these plots, negative sign(λ_2)ρ values (left side) indicate attractive interactions (hydrogen bonds, ionic coordination), values near zero (center) indicate weak van der Waals contacts, and positive values (right side) indicate repulsive steric clashes. Lower RDG values correspond to stronger interactions. In the PCE system, the scatter plot shows a broad peak centered near zero (sign(λ_2)ρ ≈ 0, RDG ≈ 0.02–0.05 a.u.), indicating predominantly weak van der Waals interactions within the molecule. A small shoulder extends into the negative region (sign(λ_2)ρ ≈ −0.01 to −0.02 a.u.), corresponding to moderate hydrogen bonding between carboxylate and ether oxygens. No positive spikes are observed, confirming the absence of repulsive steric clashes.

In PCE–SiO_2 system, the scatter plot reveals a new, more pronounced negative shoulder extending to sign(λ_2)ρ ≈ −0.03 a.u. with lower RDG values (≈0.01 a.u.), indicating stronger attractive interactions at the PCE–silica interface. The central van der Waals peak broadens, reflecting additional weak contacts along the polymer–silica interface. These changes confirm enhanced hydrogen bonding between PCE functional groups and silanol sites. In PCE–Ca^{2+}–SiO_2 system, the scatter plot shows a distinct new spike at sign(λ_2)ρ ≈ −0.04 to −0.05 a.u. with RDG values approaching zero. This corresponds to very strong attractive interactions—specifically, ionic coordination between Ca^{2+} and carboxylate oxygens. The central van der Waals peak remains but is diminished relative to the ionic spike. No positive sign(λ_2)ρ values appear, confirming a stable, non-repulsive intermolecular network.

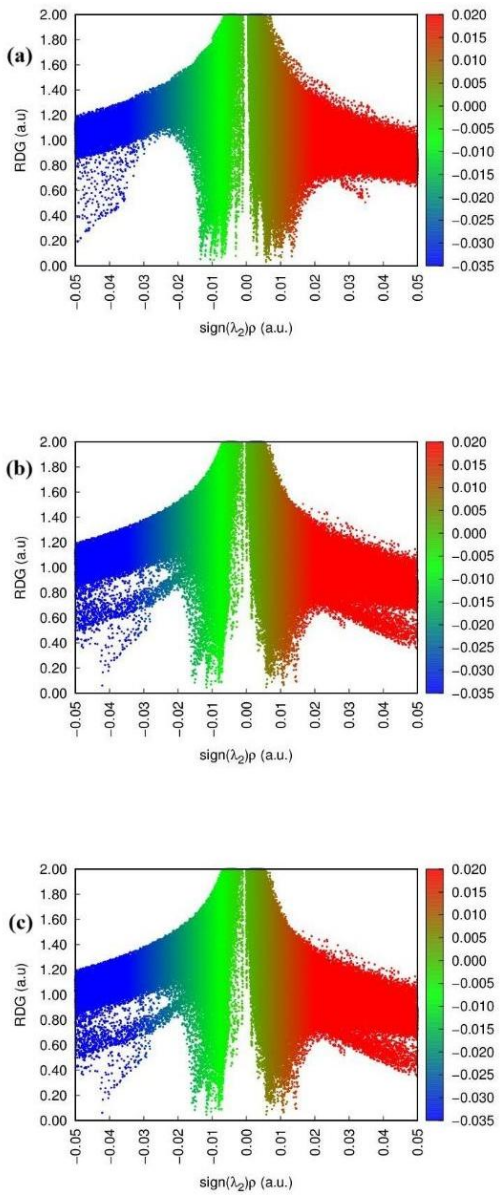

Figure 5. RDG for PCE superplasticizer (a), PCE superplasticizer with SiO_2 (b), and PCE superplasticizer with calcium and SiO_2 (c). Axis labels (RDG vs. sign(λ_2)ρ) with thresholds at –0.04, 0, and +0.04 a.u. and blue (attractive, sign(λ_2)ρ < –0.02), green (van der Waals, –0.02 to 0.02), red (repulsive, >0.02).

RDG quantifies the strength distribution of all non-covalent interactions in a single plot, distinguishing weak van der Waals (center) from strong attractive (negative) and repulsive (positive) interactions. Unlike NCI (spatial mapping) or QTAIM (precise BCP values), RDG provides a global, semi-quantitative overview of interaction strengths across the entire system. Quantitative QTAIM analysis (See Table 4) of the PCE–Ca^{2+}–SiO_2 system reveals bond critical points (BCPs) with electron densities ρ(r) ranging from 0.435 to 0.453 e/bohr^3 and Laplacian values $\nabla^2\rho(r)$ from −25.8 to −27.0 e/bohr^5. These values are characteristic of strong closed-shell ionic interactions, specifically Ca^{2+}–O coordination bonds. In contrast, BCPs in the PCE-only system exhibit ρ(r) values an order of magnitude lower (0.01–0.08 e/bohr^3), quantitatively confirming that the presence of Ca^{2+} ions dramatically enhances the binding affinity of PCE carboxylate groups.

The consistent ρ(r) values across multiple BCPs (CP 2, 4, 5, 6, 13, 19, 21, 23, 25, 30) further indicate a stable and well-defined coordination environment at the PCE–Ca^{2+}–SiO_2 interface.

Table 4. Quantitative QTAIM descriptors for selected bond critical points (BCPs) in the PCE–Ca^{2+}–SiO_2 system

CP #	ϱ(r) (e/bohr³)	∇²ϱ(r) (e/bohr⁵)	sign(λ₂)ϱ (e/bohr³)
CP 2 (3; -3)	0.441	-26.30	-0.441
CP 4 (3; -3)	0.442	-26.39	-0.442
CP 5 (3; -3)	0.435	-25.85	-0.435
CP 6 (3; -3)	0.441	-26.35	-0.441
CP 13 (3; -3)	0.444	-26.49	-0.444
CP 19 (3; -3)	0.446	-26.66	-0.446
CP 21 (3; -3)	0.453	-27.02	-0.453
CP 23 (3; -3)	0.442	-26.37	-0.442
CP 25 (3; -3)	0.435	-25.90	-0.435
CP 30 (3; -3)	0.441	-26.34	-0.441

3.4 ELF maps

Figure 6 presents ELF maps for the three systems. While MEP maps electrostatic potential, NCI visualizes interaction zones, and RDG quantifies interaction strength distributions, ELF specifically reveals the degree of electron localization—distinguishing covalent/ionic bonding (ELF → 1) from metallic/delocalized (ELF → 0.5) and van der Waals/vacuum regions (ELF → 0). ELF is particularly useful for identifying the electronic character of coordination bonds. In the PCE system, high ELF values (≈0.95–0.99) surround the oxygen atoms of carboxylate (–COO^-) and ether (–O–) groups, corresponding to lone-pair electrons localized on these electronegative atoms. Lower ELF values (≈0.3–0.5) along the carbon backbone indicate delocalized σ-electrons. This distribution confirms that the oxygen lone pairs are the primary sites for future coordination with cations. In the PCE–SiO_2 system, ELF maps show enhanced localization at the PCE–silica interface. High ELF regions (≈0.95–0.98) appear between silanol (–SiOH) oxygens and PCE carboxylate/ether oxygens. This indicates hydrogen bond formation with strong localized electron density shared between the interacting oxygens, supporting physical adsorption of PCE onto micro-silica.

In PCE–Ca^{2+}–SiO_2 system, the ternary system exhibits the most distinctive ELF features. Extremely high ELF values (≈0.99–1.00) appear directly between Ca^{2+} ions and carboxylate oxygens, confirming closed-shell ionic coordination rather than covalent bonding. Notably, ELF between Ca^{2+} and the silica surface is slightly lower (≈0.90–0.95), indicating a weaker but still substantial interaction. The preservation of high ELF around carboxylate oxygens after Ca^{2+} coordination confirms that the ionic bond does not fully deplete the electron lone pairs, leaving some capacity for additional interactions. ELF uniquely determines the electronic character of interactions, distinguishing ionic coordination (ELF ≈ 1.0 with localized electron density on both partners) from covalent bonding (ELF ≈ 1.0 with shared density along the bond axis) and from weak van der Waals contacts (ELF ≈ 0). Unlike NCI (which colors all attractive interactions blue) or QTAIM (which requires BCP analysis), ELF provides an immediate visual indicator of bond type and electron localization degree.

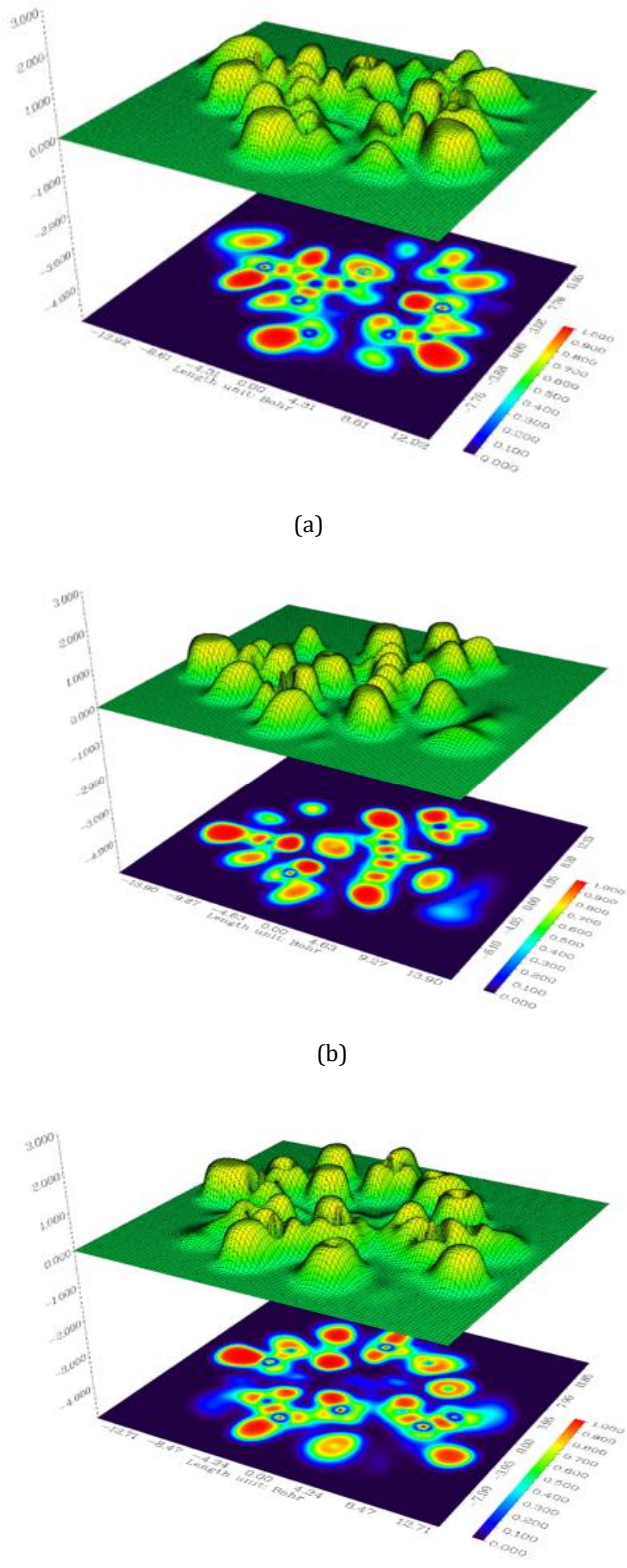

(a)

(b)

Figure 6. ELF for PCE superplasticizer (a), PCE superplasticizer with SiO2 (b), and PCE superplasticizer with calcium and SiO2 (c). Color scale bar (0.0 to 1.0) with isovalue contour = 0.75 for localization surfaces

3.5 Critical points

Figure 7 presents the critical point topological analysis derived from Quantum Theory of Atoms in Molecules (QTAIM) for three molecular systems: (a) the standalone PCE (polycarboxylate ether) superplasticizer, (b) the PCE superplasticizer interacting with micro-silicon (SiO_2), and (c) the PCE superplasticizer in the presence of both calcium ions (Ca^{2+}) and micro-silicon. Figure 7 presents QTAIM critical point topologies for the three systems, and Table 4 provides quantitative descriptors for selected bond critical points (BCPs) in the PCE–Ca^{2+}–SiO_2 system. While MEP maps electrostatics, NCI visualizes interaction zones, RDG quantifies strength distributions, and ELF reveals electron localization character, QTAIM uniquely provides precise, quantitative bond descriptors at critical points, including electron density ρ(r), Laplacian $\nabla^2\rho(r)$, bond ellipticity, and interaction energy estimates.

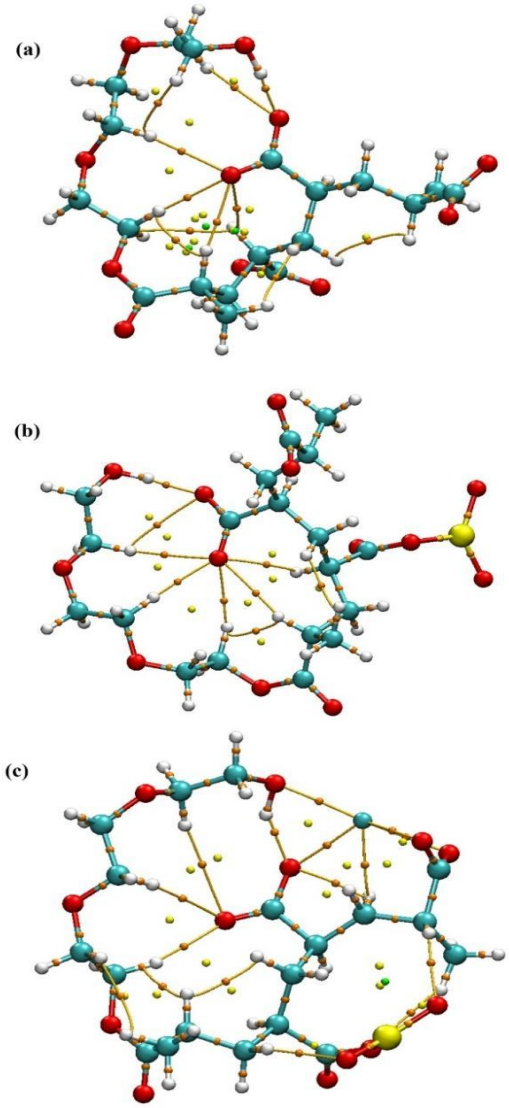

Figure 7. Critical points for PCE superplasticizer (a), PCE superplasticizer with SiO2 (b), and PCE superplasticizer with calcium and SiO2 (c). Critical point types (BCP = green sphere, RCP = orange sphere, CCP = red sphere) with bond paths as gray lines

In the PCE system, the topology shows dispersed bond critical points (BCPs, green spheres) and ring critical points (RCPs, orange spheres) primarily around carboxylate and ether oxygen atoms. These BCPs exhibit low electron densities (ρ(r) ≈ 0.01–0.08 e/bohr^3, data not shown), characteristic of weak intramolecular hydrogen bonds and van der Waals contacts. This sparse topology confirms the absence of strong intramolecular interactions in the isolated superplasticizer. In the PCE–SiO_2 system, additional BCPs emerge at the PCE–silica interface, specifically between silanol oxygens and PCE carboxylate/ether groups. The increased number of BCPs (approximately double relative to isolated PCE) and the formation of new RCPs indicate a more connected intermolecular network. These BCPs exhibit intermediate ρ(r) values (≈0.10–0.20 e/bohr^3), confirming hydrogen-bond strength interactions. In the PCE–Ca^{2+}–SiO_2 system, the ternary system exhibits the most complex and dense topology. Table 4 presents quantitative QTAIM descriptors for representative BCPs (CP 2, 4, 5, 6, 13, 19, 21, 23, 25, 30), all of type (3,-3)- true bond critical points.

It should be noted that solvent effects were not included in the present DFT calculations. In real cement pore solutions, water molecules may influence ion coordination, hydrogen-bonding networks, and adsorption behavior. Therefore, the reported interactions should be interpreted as fundamental gas-phase interactions. Future studies employing implicit solvent models (PCM or SMD) and explicit water molecules will provide a more realistic description of the cementitious environment.

3.6 Forecasting of greenhouse gas emissions analysis

This study adopts a molecular-to-scenario translation framework to link the DFT results with the WAM emission scenario. The DFT results indicate that the PCE–Ca^{2+}–SiO_2 system has a denser coordination network compared to the isolated systems of PCE and PCE–SiO_2. In particular, the Ca^{2+} ion forms additional coordination contacts with the carboxylate oxygen atoms and with SiO_2. The model offers oxygen-containing interaction sites. This helps justify the mechanistic plausibility of enhanced adsorption and dispersion in cementitious systems containing silica fume. The DFT calculations, however, do not directly calculate the clinker reduction and national greenhouse gas mitigation. Rather, the molecular findings are used to argue for the technological feasibility of the WAM assumption that optimized PCE–silica-fume systems can achieve lower clinker/cement levels without compromising workability and performance. So, the quantitative clinker/cement reduction parameter in the WAM scenario is based on the literature and the roadmap's assumptions, not directly on DFT energies. Clinker substitution is a key decarbonization lever for the Kazakhstan cement sector, as identified in a previous roadmap analysis, in which the clinker content is reduced to 75% in the medium case and 70% in the rapid case by 2030. It is also found that the dosage of silica fume and superplasticizer significantly influences the workability, mechanical strength, and microstructure of silica-fume and polycarboxylate-superplasticizer systems through experimental studies.

The WAM scenario is therefore based on an 80% share of mineral-industry emissions from cement, a clinker-to-cement ratio of 10% for adopted PCE–silica-fume mixes, and a 70% adoption rate by 2040. These assumptions result in an effective additional reduction of 5.6% compared to the WCM mineral-industry pathway in 2040. Thus, DFT is used to provide mechanistic support for the feasibility of the

material-efficiency pathway, whereas the emission reduction is calculated using the scenario model. The actual and forecasted CO_2 equivalent emission rates in Kazakhstan for the period of 1990-2040, for three scenarios, WOM, WCM, and WAM, are presented in Figure 8. The data demonstrate a definite tendency of rising emissions in all the scenarios, though with various rates. The period 1990 to 2022 (fact years) shows early changes in emissions as economies undergo change following the collapse of the Soviet Union, after which emissions increase consistently with industrial growth and urbanization [29, 30].

In the WOM scenario, emissions rise significantly, suggesting a business-as-usual approach with no restrictions or other emission-reducing actions to offset the emissions from traditional cement production methods. This situation is the most emissions-intensive due to the continued use of clinker-intensive technologies and the inefficiency of concrete production. The current regulatory and technological environment, as embodied in the WCM scenario, shows a moderate decrease in emission growth compared to WOM. This is due to the gradual increase in cement production efficiency and the low use of additional cementitious materials. This is in line with the current policy direction in Kazakhstan, which emphasizes improving energy efficiency but does not extend to broader reforms of the energy sector.

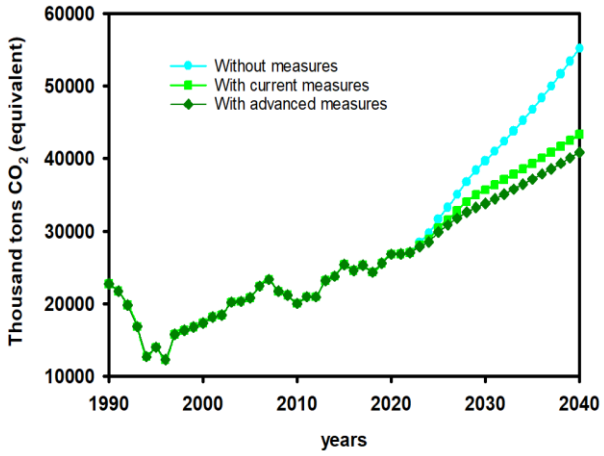

Figure 8. Actual and forecasted emission levels

The WAM scenario is the most sustainable route and involves partial substitution of cement with polycarboxylate superplasticizers and silica fume, among other elaborate steps. The WAM emission rate is much lower, indicating the combined impact of reducing clinker content, improving cement efficiency, and using innovative materials. This is the lowest-emission scenario by 2040, highlighting how material innovations can help decarbonize the concrete industry. These findings can be explained by previous DFT studies that have established stronger molecular interactions between polycarboxylate superplasticizers and cementitious substances, thereby allowing a significant decrease in clinker content without affecting, and even improving, mechanical properties. The above scenario results are consistent with the anticipated results of the National Roadmap, which advocates banning new wet-process cement facilities and imposing an import carbon levy (Measure 4). In the transition to more efficient production processes and at least partial replacement of coal with municipal solid waste, the roadmap forecasts that investments of about 30 million USD will be needed in 2026-2030 [28]. Projections indicate that policy interventions and the adoption of modern measures are urgently needed to achieve significant reductions in emissions. Under WOM, emissions will grow by more than 60% between 2023 and 2040, compared to 50% under WCM and 35% under WAM, which reduces emissions by the largest percentages. Figure 9 depicts the mineral industry's emissions in Kazakhstan for the period 2030-2040 across three cases: WOM, WCM, and WAM.

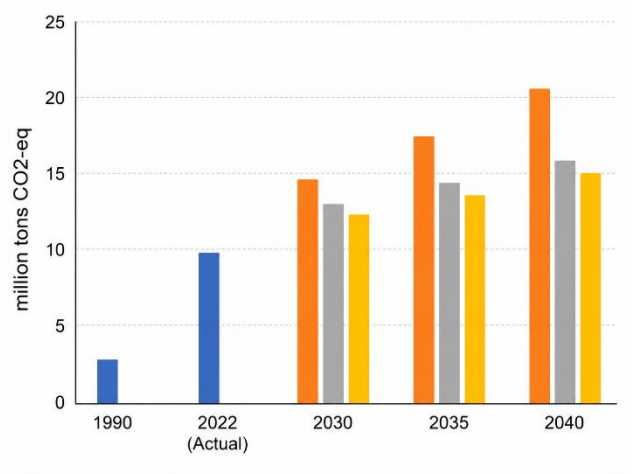

Figure 9. Emissions in the Mineral industry by scenario until 2040, million tons CO_2-eq

Due to a lack of information on actual PCE dosage, silica fume availability, the clinker factor, and technology adoption among all cement producers in Kazakhstan, the WAM scenario was tested using a simple sensitivity analysis. The sensitivity analysis is performed considering three parameters: the adoption rate of PCE–silica-fume A(2040), the fraction of clinker/cement reduction Rclinker, and the share of mineral-industry emissions related to cement Scement. The 2040 WCM mineral-industry value of 15.86 Mt CO_2-eq was used as the reference pathway (Table 5). The mineral industry is still the largest emitter in the IPPU sector. In the WOM scenario, emissions from this subsector rise significantly, from 14.60 Mt in 2030 to 20.59 Mt in 2040, reflecting ongoing industrial development without mitigation. In contrast, the WCM scenario has lower emissions of 15.86 Mt in 2040, due to limited mitigation efforts. The WAM scenario is the one with the largest emission reduction, as emissions are limited to 14.97 Mt in 2040 by using advanced materials, such as polycarboxylate superplasticizers, that reduce clinker content and the associated CO_2 emissions from cement manufacturing.

Emissions are also generated by the chemical industry. In the WOM scenario, its emissions increase from 0.83 million tons in 2030 to 1.17 million tons in 2040. The WCM scenario limits this increase to 0.90 Mt in 2040, while the WAM scenario further reduces emissions to 0.82 Mt through optimized chemical processes and material substitution. The metal industry, another major emitter, shows a clear upward trend in emissions, from 21.03 Mt in 2030 to 29.66 Mt in 2040 under the WOM scenario. Even though emissions from non-energy products, driven by fuel and solvent consumption, are not large, they grow under the WOM scenario to 0.24 Mt in 2030 and 0.33 Mt in 2040.

Table 5. Sensitivity of 2040 mineral-industry emissions to WAM assumptions

Case	A(2040), adoption rate	Rclinker, clinker /cement reduction	Sce-ment	Calculated 2040 mineral-industry emissions, Mt CO_2-eq	Reduction vs WCM, MtCO_2eq
Conser-vative	40%	5%	70%	15.64	0.22
Base	70%	10%	80%	14.97	0.89
Ambitious	80%	12%	85%	14.57	1.29

Table 6. Comparison with prior DFT studies and cement decarbonization roadmaps

Study	Focus	Methodology	Connection to Emission Reduction
Plank et al. (2010) [16]	PCE intercalation into C_3A hydrate phases	Experimental + DFT	None
Yamada et al. (2000) [18]	Chemical structure vs. PCE properties	Experimental	None
Jamil et al. (2020) [8]	Acrylate-PEG copolymers on C-S-H surfaces	DFT/MD	None
Šoukal et al. (2023) [17]	Silica fume and superplasticizer in RPC	Experimental	Qualitative only
EBRD Roadmap (2016) [7]	Low-carbon cement industry in Kazakhstan	Policy/ technology scenarios	Macro-scale only
UNFCCC NID (2024) [28]	GHG inventory for Kazakhstan	Statistical	Macro-scale only
This work	PCE–Ca^{2+}–SiO_2 interactions + IPPU emission forecasts	DFT-QTAIM + scenario modeling	Quantitative (ρ(r) → clinker reduction → 35% CO_2 mitigation)

WCM only minimizes these emissions to 0.26 Mt, whereas WAM minimizes them to 0.24 Mt by incorporating cleaner production technologies. ODS use as a substitute for products also increases in each of the WOM scenarios, reaching 2.98 Mt in 2030 and 3.46 Mt in 2040. WCM does not reduce emissions compared to WOM, whereas WAM reduces them to 3.17 Mt in 2040, benefiting from more stringent regulations. Remarkably, the other product manufacturing category captures no substantial emissions in all situations, highlighting its insignificant contribution to the industry. As a whole, the IPPU sector carbon emissions in the WOM scenario increase 39.68 Mt in 2030 and reach 55.21 Mt in 2040, illustrating the effects of unregulated industry-related carbon emissions. This growth is minimized in the WCM scenario, where emissions are 43.34 Mt in 2040, whereas the WAM scenario shows the greatest mitigation, with capped emissions at 40.87 Mt. These results demonstrate the essential role of taking high-tech steps to decarbonize industry. The use of new technologies, material replacements, and energy-saving processes can significantly reduce emissions and help the IPPU industry in Kazakhstan comply with national and global climate goals. Strong governmental frameworks and business commitment will be required to achieve these reductions [31,32].

Although many DFT and molecular dynamics (MD) studies have explored PCE interactions with cement phases (Table 6), few have examined molecular-level mechanisms and linked them to the potential for emission reduction at the macroscopic scale. On the other hand, current cement decarbonization roadmaps for Kazakhstan and other emerging economies have suggested clinker substitution but have failed to provide atomistic evidence for the preference for certain additives (e.g., PCE with silica fume). The core novelty and importance of this study lies in bridging this gap, which we combine quantitative DFT-QTAIM analysis of PCE–Ca^{2+}–SiO_2 interactions with scenario-based GHG emission forecasting for the Industrial Processes and Product Use (IPPU) sector of Kazakhstan. To our knowledge, this is one of the first studies to combine DFT-based analysis of PCE–Ca^{2+}–SiO_2 interactions with a Kazakhstan-specific IPPU emission scenario framework. The study does not claim that molecular descriptors directly determine national CO_2 reductions. Rather, it uses molecular evidence to support the technological plausibility of PCE–silica-fume material-efficiency assumptions, while the emission reduction values are generated by the scenario model. This integrated approach is particularly relevant for Kazakhstan, where cement production remains a major and growing source of emissions, and where policymakers require science-based justifications for material substitution strategies.

3.7 Environmental and practical implications

Thus, the use of PCE–silica-fume cement systems should be considered a mix-design optimization problem rather than a universal cement-replacement rule. Dosage depends on cement composition, silica fume fineness, sulfate balance, alkali content, water-cement ratio, mixing sequence, curing conditions, and desired strength class. According to the literature on RPC, the amounts of silica fume and polycarboxylate superplasticizer can be significant factors in the slump flow, density, compressive strength, flexural strength, and microstructure of RPC, with an optimum system being 3.5-4.0% superplasticizer and 15-25% silica fume. The values should not be mechanically applied to regular concrete; rather, they indicate that the dosage of PCE–silica fume should be determined experimentally for each binder system. The material-efficiency pathway assumed in the WAM scenario is conservative, meaning the model does not fully assume the substitution of cement with admixtures. Instead, it assumes that optimized use of PCE–silica fume enables a 10% reduction in clinker/cement content in adopted mixes, due to improved dispersion, workability, and greater utilization of supplementary cementitious materials. This value is to be used as a scenario parameter and needs to

be verified through laboratory and plant-scale tests prior to industrial application. Scalability and cost are also important factors. PCE superplasticizers are more expensive, and their availability depends on local and regional supply from the silicon and ferrosilicon industries. Feasibility in Kazakhstan may be affected by transport costs, consistency of quality, densification, storage, and dispersion of silica fume. Workability loss, the need for additional water, delayed or modified hydration, and sensitivity to superplasticizer type may occur at high silica-fume contents. Hence, the advantages of clinker reduction should be weighed against early-age strength, setting time, pumpability, shrinkage, durability, and long-term performance.

The real cement pore solution is not fully captured by the DFT model employed in this work. The −3 charge state is a chemically reasonable approximation to the alkaline limit, and the molecular fragment is not a full commercial PCE polymer. Explicit water, high ionic strength, alkali ions, sulfates, aluminates, C_3S, C_2S, and C-S-H phases are also not included in the model. Thus, the DFT results are not meant to be used as a direct measure of concrete performance, but rather as a mechanism for local PCE–Ca^{2+}–SiO_2 coordination. It is recommended that future work be carried out in conjunction with adsorption tests, zeta-potential measurements, rheology, calorimetry, compressive strength tests, durability testing, and Kazakhstan-specific cost and supply chain analysis.

4. Conclusion

In this work, DFT-based atomistic analysis and GHG emission forecasting were employed to assess the potential contribution of silica-fume cement systems with PCE in the decarbonization of Kazakhstan's industry. The DFT results indicated that carboxylate oxygen atoms in the PCE fragment can form Ca^2+-mediated coordination contacts in the presence of SiO_2, suggesting that adsorption and dispersion may be enhanced in silica-rich cementitious environments. The scenario analysis indicates that further actions are needed to slow the growth of Kazakhstan's IPPU emissions. The material-efficiency assumptions, combined with current policy measures, result in the strongest mitigation pathway in the WAM scenario by 2040 compared with the WOM scenario. The reductions are not the direct result of DFT calculations, but rather the result of scenario modeling based on assumptions about adoption, clinker reduction, and cement-related emission factors. The study thus provides a molecularly based framework to assess green cement production technologies. The analysis connects the mechanisms of interaction between PCE and Ca^2+-SiO_2 with assumptions for transparent emission scenarios, thereby enabling a more evidence-based discussion of options for decarbonizing the cement industry in Kazakhstan. There are some limitations to consider. The DFT model does not contain C_3S, C_2S, C-S-H, aluminates, sulfates, alkali ions, explicit water, or high pore-solution ionic strength, but rather utilizes a simplified PCE fragment, a minimal SiO_2 representation, and Ca^{2+} as a reduced cementitious-system proxy. Future studies should use larger cement-phase models, different protonation states, both implicit and explicit solvation, and experimental validation via adsorption, rheology, zeta potential, compressive strength, and durability testing. The integrated approach is a useful starting point for future research on sustainable cementitious materials and for policy debates on reducing industrial GHG emissions, despite these limitations. Optimization of PCE dosage, silica-fume content, cost, supply availability, early-age strength, long-term durability, and scalability in the cement industry in Kazakhstan will be required for practical implementation. In the future, larger, more realistic models that include major cement phases (C_3S, C_2S, C-S-H, aluminate structures) should be used to further clarify the molecular mechanisms underlying superplasticizer adsorption and the interactions between cement and additives under practical conditions. Furthermore, further investigations should consider solvent effects using implicit solvation models (PCM/SMD) and explicit water molecules to more accurately mimic the highly aqueous conditions of cement pore solutions and to further confirm the adsorption mechanism found in this study. Use of atomistic simulations and emissions predictions offers a holistic solution to building industry environmental issues. This publication serves as a starting point for additional research on sustainable materials and reminds of the need for additional innovation and policy measures to reduce the amount of greenhouse gases in Kazakhstan and other countries.

Acknowledgements

This research was funded by the Ministry of Science and Higher Education of the Republic of Kazakhstan (Grant No. AP23490690). The DFT calculations were performed at L.N. Gumilyov Eurasian National University.

Ethical issue

The authors are aware of and comply with best practices in publication ethics, specifically regarding authorship (avoidance of guest authorship), dual submission, manipulation of figures, competing interests, and compliance with research ethics policies. The authors adhere to publication requirements that the submitted work is original and has not been published elsewhere.

Data availability statement

The manuscript contains all the data. However, additional data will be provided by the corresponding author upon reasonable request.

Conflict of interest

The authors declare no potential conflict of interest.

References

[1] Zhakiyev, N., Sagadatova, N., Ismagulova, G., Bakdolotov, A., & Biloshchytskyi, A. (2024). Hybrid technico-economical modeling of the mid-term green economy and low-carbon development strategy of Kazakhstan. ES Energy and Environment, 25, 1235. DOI: https://doi.org/10.30919/esee1235

[2] United Nations Climate Change. (2020). National inventory report: Kazakhstan on the anthropogenic greenhouse gas emissions for 1990–2018. Bonn, Germany: UNFCCC. URL: https://unfccc.int/documents/253715

[3] United Nations Framework Convention on Climate Change. (2012). Doha Climate Change Conference. Doha, Qatar. URL: https://unfccc.int/process-and-meetings/conferences/pastconferences/doha-climate-change-conference-november-2012/doha-climate-change-conference-november-2012

[4] United Nations Framework Convention on Climate Change. (2015). The Paris Agreement. Paris, France. URL: https://unfccc.int/process-and-meetings/the-paris-agreement

[5] Zhakiyev, N., Akhmetov, Y., Omirgaliyev, R., et al. (2024). Comprehensive scenario analyses for coal exit and renewable energy development planning of Kazakhstan using PyPSA-KZ. Engineered Science, 29, 1085. DOI: https://doi.org/10.30919/es1085

[6] Carbone, C., Ferrario, D., Lanzini, A., Stendardo, S., & Agostini, A. (2022). Evaluating the carbon footprint of cement plants integrated with the calcium looping CO2 capture process. Frontiers in Sustainability, 3, 809231. DOI: https://doi.org/10.3389/frsus.2022.809231

[7] European Bank for Reconstruction and Development. (2016). Technology roadmap: For a sustainable low-carbon future of the Kazakhstan cement industry. London, U.K.: European Bank for Reconstruction and Development. URL: https://shiftingparadigms.nl/wp-content/uploads/2018/11/Kazakhstan-Technology-Roadmap-Low-Carbon-Cement-1.pdf

[8] Jamil, T., Javadi, A., & Heinz, H. (2020). Mechanism of molecular interaction of acrylate-polyethylene glycol acrylate copolymers with calcium silicate hydrate surfaces. Green Chemistry, 22(5), 1577–1593. DOI: https://doi.org/10.1039/C9GC03287H

[9] Deilami, S., Aslani, F., & Elchalakani, M. (2019). An experimental study on the durability and strength of SCC incorporating FA, GGBS and MS. Proceedings of the Institution of Civil Engineers - Structures and Buildings, 172(5), 327–339. DOI: https://doi.org/10.1680/jstbu.17.00129

[10] Frhaan, W. K., Bakar, H. B. A., Hilal, N., & Al-Hadithi, A. I. (2020). Effect of silica fume and super-plasticizer on mechanical properties of self-compacting concrete: A review. IOP Conference Series: Materials Science and Engineering, 978, 012052. DOI: https://doi.org/10.1088/1757-899X/978/1/012052

[11] McLellan, B. C., Williams, R. P., Lay, J., Van Riessen, A., & Corder, G. D. (2011). Costs and carbon emissions for geopolymer pastes in comparison to ordinary Portland cement. Journal of Cleaner Production, 19(9-10), 1080–1090. DOI: https://doi.org/10.1016/j.jclepro.2011.02.010

[12] Scrivener, K. L., & Nonat, A. (2011). Hydration of cementitious materials, present and future. Cement and Concrete Research, 41(7), 651–665. DOI: https://doi.org/10.1016/j.cemconres.2011.03.026

[13] Tripathi, N., Hills, C. D., Singh, R. S., Kyeremeh, S., & Hurt, A. (2024). Mineralisation of CO2 in wood biomass ash for cement substitution in construction products. Frontiers in Sustainability, 5, 1287543. DOI: https://doi.org/10.3389/frsus.2024.1287543

[14] Al-Hadithi, A. I., Noaman, A. T., & Mosleh, W. K. (2019). Mechanical properties and impact behavior of PET fiber reinforced self-compacting concrete (SCC). Composite Structures, 224, 111021. DOI: https://doi.org/10.1016/j.compstruct.2019.111021

[15] Mohammed, M. K., Al-Hadithi, A. I., & Mohammed, M. H. (2019). Production and optimization of eco-efficient self-compacting concrete with limestone and PET. Construction and Building Materials, 197, 734–746. DOI: https://doi.org/10.1016/j.conbuildmat.2018.11.189

[16] Plank, J., Zhimin, D., Keller, H., Hössle, F. V., & Seidl, W. (2010). Fundamental mechanisms for polycarboxylate intercalation into C3A hydrate phases and the role of sulfate present in cement. Cement and Concrete Research, 40(1), 45–57. DOI: https://doi.org/10.1016/j.cemconres.2009.08.013

[17] Šoukal, F., Bocian, L., Novotný, R., Dlabajová, L., Šuleková, N., Hajzler, J., Koutný, O., & Drdlová, M. (2023). The effects of silica fume and superplasticizer type on the properties and microstructure of reactive powder concrete. Materials, 16(20), 6670. DOI: https://doi.org/10.3390/ma16206670

[18] Yamada, K., Takahashi, T., Hanehara, S., & Matsuhisa, M. (2000). Effects of the chemical structure on the properties of polycarboxylate-type superplasticizer. Cement and Concrete Research, 30(2), 197–207. DOI: https://doi.org/10.1016/S0008-8846(99)00230-6

[19] Khaiyum, M. Z., Sarker, S., & Kabir, G. (2023). Evaluation of carbon emission factors in the cement industry: An emerging economy context. Sustainability, 15(21), 15407. DOI: https://doi.org/10.3390/su152115407

[20] Assylbekov, D., Nadeem, A., Hossain, M. A., Akhanova, G., & Khalfan, M. (2021). Factors influencing green building development in Kazakhstan. Buildings, 11(12), 634. DOI: https://doi.org/10.3390/buildings11120634

[21] Gregory, J., AzariJafari, H., Vahidi, E., Guo, F., Ulm, F.-J., & Kirchain, R. (2021). The role of concrete in life cycle greenhouse gas emissions of US buildings and pavements. Proceedings of the National Academy of Sciences of the United States of America, 118(37), e2021936118. DOI: https://doi.org/10.1073/pnas.2021936118

[22] Becke, A. D. (1996). Density-functional thermochemistry. IV. A new dynamical correlation functional and implications for exact-exchange mixing. Journal of Chemical Physics, 104, 1040–1046. DOI: https://doi.org/10.1063/1.470829

[23] Lee, C., Yang, W., & Parr, R. G. (1988). Development of the Colle-Salvetti correlation-energy formula into a functional of the electron density. Physical Review B, 37, 785–789. DOI: https://doi.org/10.1103/PhysRevB.37.785

[24] Harrison, J. A., Schall, J. D., Maskey, S., Mikulski, P. T., Knippenberg, M. T., & Morrow, B. H. (2018). Review of force fields and intermolecular potentials used in atomistic computational materials research. Applied Physics Reviews, 5(3). DOI: https://doi.org/10.1063/1.5020808.

[25] Rakhimbayev, B., Mukashev, B., Kusherova, P., Serikkanov, A., Kemelbekova, A., Agybayev, K., Aldongarov, A., & Almas, N. (2024). Atomistic Insight on Effect of Silica Fume on Intermolecular Interactions between Poly(carboxylate) Superplasticizer and Calcium Ions in Concrete. Nanomaterials, 14(13), 1084. DOI: https://doi.org/10.3390/nano14131084

[26] Lu, T., & Chen, F. (2012). Multiwfn: A multifunctional wavefunction analyzer. Journal of Computational

Chemistry, 33(5), 580–592. DOI: https://doi.org/10.1002/jcc.22885

[27] Humphrey, W., Dalke, A., & Schulten, K. (1996). VMD: Visual molecular dynamics. Journal of Molecular Graphics, 14(1), 33–38. DOI: https://doi.org/10.1016/0263-7855(96)00018-5

[28] United Nations Framework Convention on Climate Change. Kazakhstan. National Inventory Document (NID). Publication date: 30 December 2024. UNFCCC Documents Database. Available at: https://unfccc.int/documents/645161

[29] Zhakiyev, N. K., Kayisli, K., Kushekkaliyev, A., Sagadatova, N., & Biloshchytskyi, A. (2025). Forecasting of GHG emissions from energy and industrial sectors of Kazakhstan and assessment of mitigation scenarios with high share of renewables. International Journal of Renewable Energy Research, 15(2), 300–309. DOI: https://doi.org/10.20508/ijrer.v15i2.15837.g9052

[30] Gökçekuş, H., Kassem, Y., & Andaque, H. H. S. (2023). Interaction between infrastructure and climate change on buildings, roads, and bridges in developed and developing countries: a case of Japan and Mozambique. Future Technology, 2(3), 24–30. DOI: https://doi.org/10.55670/fpll.futech.2.3.5

[31] Government of the Republic of Kazakhstan. Action Plan for the Implementation of the Concept for the Transition of the Republic of Kazakhstan to a Green Economy for 2024–2030. Approved by Government Decree No. 1019 of 29 November 2024. URL: https://adilet.zan.kz/kaz/docs/P2400001019 (in Kazakh language).

[32] Khamzina, A., Ten, A., Mukatov, B., et al. (2025). Critical Analysis of Tariff Policy and Legislative Measures for Renewable Energy Development: Medium-Term Challenges and Prospects of Kazakhstan.ES Energy & Environment. 28, 1560. DOI: http://dx.doi.org/10.30919/ee1560